

# Global scrape-off layer electromagnetic fluid turbulence simulations

F.D. Halpern, S. Jolliet, J. Loizu, A. Masetto, P. Ricci

École Polytechnique Fédérale de Lausanne  
Centre de Recherches en Physique des Plasmas  
Association Euratom-Confédération Suisse  
CH-1015 Lausanne, Suisse

September 3rd, 2012

# Outline

Introduction

Model

Global SOL simulations

Discussion

- Non linear saturation mechanism

- Electromagnetic global mode onset

- Resistive global mode onset

Conclusions

## Motivation

- ▶ For the development of fusion, it is essential to understand :
  - ▶ Instabilities relevant to tokamak scrape-off layer (SOL)
  - ▶ Mechanisms responsible for SOL turbulent transport regimes
  - ▶ Steady-state profiles and their typical scale lengths

## SOL turbulence : interplay between $\beta$ , $\nu$ , and $\omega_*$

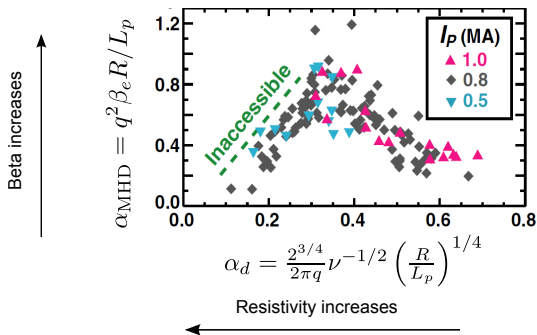
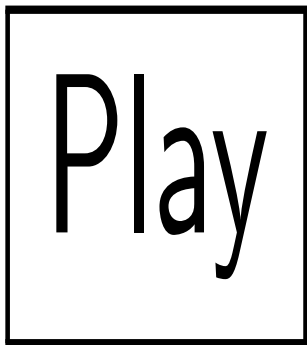


Figure : LaBombard *et al.*, *Nucl Fusion* 45, 1658 (2005)

Our goal : understanding SOL turbulence dependence on  $\beta$  and  $\nu$

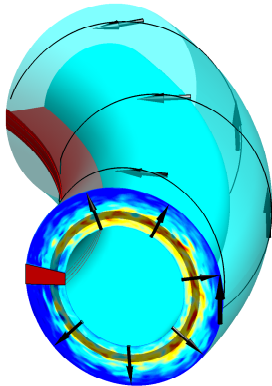
## Scrape off-layer turbulence : a challenge for modeling



- ▶ Large fluctuations respect to background density
- ▶ No separation between equilibrium and turbulent scales
- ▶ Parallel losses due to presence of open field lines

## Our approach : 3D global fluid electromagnetic simulations

- ▶ SOL *global* power balance between
  - ▶ Plasma outflow from the core
  - ▶ Perpendicular turbulent fluxes
  - ▶ Parallel losses at the limiter
- ▶ No separation between fluctuations and background quantities
- ▶ Gradient length  $L_p = -\rho/\nabla\rho$  is a simulation **result**
  - ▶ Turbulence drive ( $R/L_p$ ) is a *priori* unknown



## Model equations

Drift-reduced Braginskii equations in  $\hat{s} - \alpha$  geometry,  $T_i \ll T_e$

$$\begin{aligned} \partial_t n &= -\frac{R}{B} [\phi, n] + \frac{2}{B} [\hat{C}(p_e) - n\hat{C}(\phi)] - \nabla_{\parallel} (nv_{\parallel e}) + S_n \\ \partial_t \omega &= -\frac{R}{B} [\phi, \omega] + \frac{2B}{n} \hat{C}(p_e) - v_{\parallel i} \nabla_{\parallel} \omega + \frac{B^2}{n} \nabla_{\parallel} j_{\parallel} + \frac{B}{3n} \hat{C}(G_i) \\ \partial_t \chi &= -\frac{R}{B} [\phi, v_{\parallel e}] - v_{\parallel e} \nabla_{\parallel} v_{\parallel e} + \frac{mi}{me} \left\{ -\nu \frac{j_{\parallel}}{n} + \nabla_{\parallel} \phi - \frac{1}{n} \nabla_{\parallel} p_e - 0.71n \nabla_{\parallel} T_e - \frac{2}{3n} \nabla_{\parallel} G_e \right\} \\ \partial_t v_{\parallel i} &= -\frac{R}{B} [\phi, v_{\parallel i}] - v_{\parallel i} \nabla_{\parallel} v_{\parallel i} - \frac{1}{n} \nabla_{\parallel} p_e - \frac{2}{3n} \nabla_{\parallel} G_i \\ \partial_t T_e &= -\frac{R}{B} [\phi, T_e] - v_{\parallel e} \nabla_{\parallel} T_e + \frac{4}{3} \frac{T_e}{B} \left[ \frac{7}{2} \hat{C}(T_e) + \frac{T_e}{n} \hat{C}(n) - \hat{C}(\phi) \right] + S_{T_e} \\ &\quad + \frac{2}{3} T_e \left[ 0.71 \nabla_{\parallel} v_{\parallel i} - 1.71 \nabla_{\parallel} v_{\parallel e} + 0.71 \left( \frac{v_{\parallel i} - v_{\parallel e}}{n} \right) \nabla_{\parallel} n \right] \end{aligned}$$

with ancillary equations  $\omega = \nabla_{\perp}^2 \phi$ ,  $\chi = v_{\parallel e} + \frac{mi}{me} \frac{\beta_e}{2} \psi$ ,  $j_{\parallel} = n(v_{\parallel i} - v_{\parallel e})$ ,  $\nabla_{\perp}^2 \psi = j_{\parallel}$ ,  
 parallel gradient  $\nabla_{\parallel} a = \hat{b}_0 \cdot \nabla a + \frac{\beta_e}{2} \frac{R}{B} [\psi, a]$ , and curvature operator  $\hat{C}(a) = \frac{B}{2} \left( \nabla \times \frac{\hat{b}_0}{B} \right) \cdot \nabla a$

BCs consistent with sheath physics are imposed at the limiter

## Non-linear simulations

- ▶ Simulations carried out using the GBS code
- ▶ Typical simulation parameters

$$L_y = 2\pi a = \{400, 800\}\rho_s, \quad R_0 = \{500, 1000\}\rho_s$$

$$\nu = 5 \times 10^{-3} - 0.1, \quad m_i/m_e = 200$$

$$\beta_e = 10^{-5} - 3 \times 10^{-3}$$

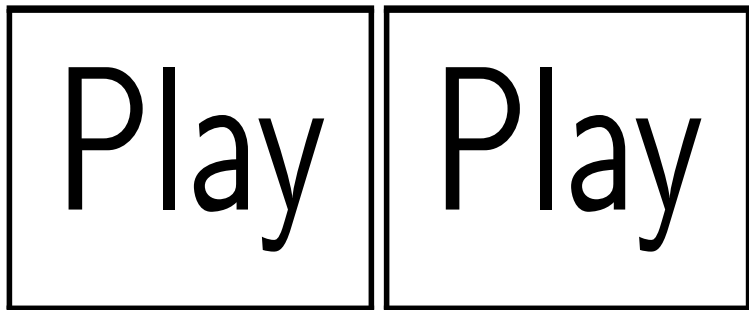
$$\hat{s} = 0, \quad q = 4$$

$$[n_x, n_y, n_z] = \{128, 256, 32\}, \{128, 512, 64\}$$

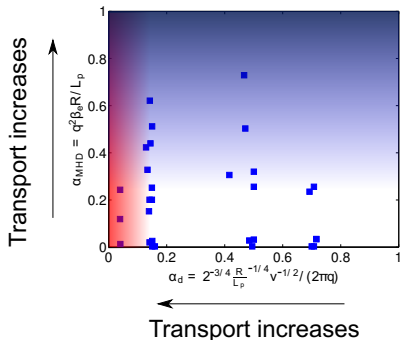
- ▶ Typically, in steady state we recover  $R/L_p \approx 10 - 20$ 
  - ▶  $\alpha_{\text{MHD}} = q^2 \beta_e R/L_p \approx 0 - 0.7$



## Non-linear turbulence driven by RBMs



## Scanned parameter space $\alpha_{\text{MHD}}$ vs $\alpha_d$



High  $\nu$ ,  $\beta_e$  lead to enhanced transport

## Equilibrium pressure gradient decreases with high $\beta_e$

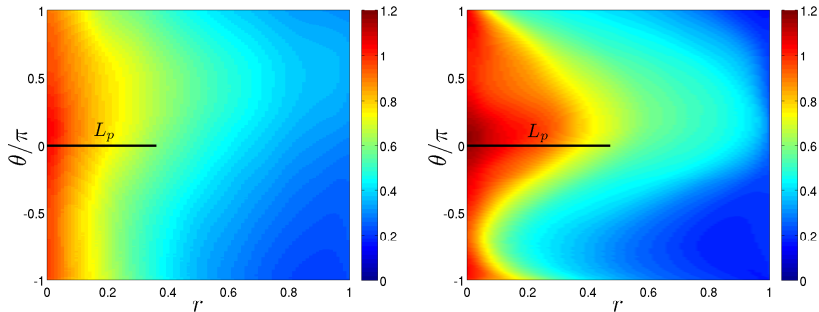


Figure :  $n_0$  for  $\alpha_{\text{MHD}} = 3 \times 10^{-3}$  (left) and  $\alpha_{\text{MHD}} = 0.7$  (right)

- ▶  $R/L_p$  can be computed from toroidal, time average of  $p_e$
- ▶ In this case  $R/L_p$  decreases  $\sim 30\%$  at high  $\beta_e$

## Turbulence changes with high $\beta_e$

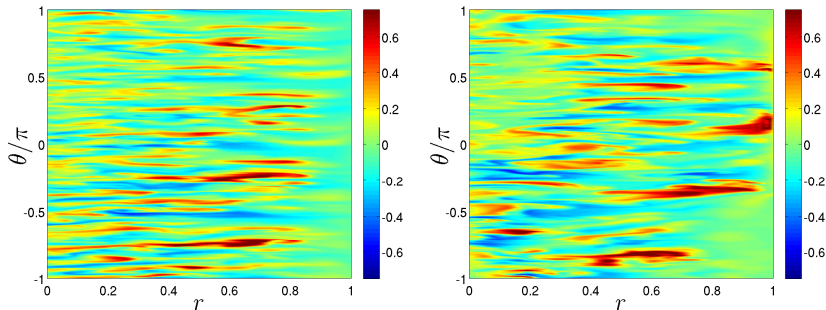


Figure :  $n_1 = (n - n_0)/n_0$  for  $\alpha_{\text{MHD}} = 3 \times 10^{-3}$  (left) and  $\alpha_{\text{MHD}} = 0.7$  (right)

- ▶ Density fluctuations of order of  $O(1)$
- ▶ Radially elongated eddies
- ▶  $k_{\theta} \rho_s$  decreases with increasing  $\beta_e$

## Turbulent spectrum changes with high $\beta_e$

Perturbed spectra shift to lower  $k_{\theta}\rho_s, n$  (global modes)

- ▶ At low  $\beta_e$ , wide spectrum with  $k_{\theta}\rho_s \approx 0.1$  dominant
- ▶ As  $\beta_e$  is increased dominant mode acquires smaller  $n, k_{\theta}\rho_s$

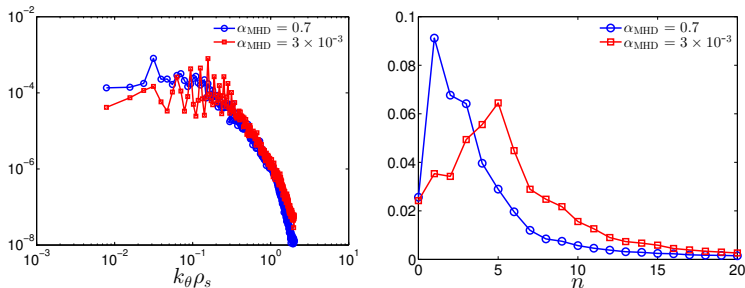
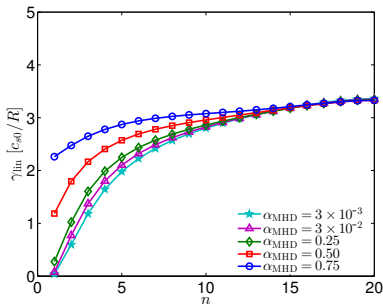


Figure :  $k_{\theta}\rho_s$  (left) and  $n$  (right) spectrum

## Linear theory does not fully explain global mode onset



- ▶  $R/L_p \approx 16$  extracted from GBS non-linear simulation
- ▶ Linear growth rates obtained with linear stability code
  - ▶ Resistive ballooning modes unstable in electrostatic limit
  - ▶ Low  $n$  ideal ballooning mode become unstable at  $\alpha_{\text{MHD}} \approx 0.25$
  - ▶ However, low  $n$  modes are still linearly sub-dominant

## Non linear saturation mechanism

We expect turbulence to saturate when its drive ( $R/L_p$ ) is removed

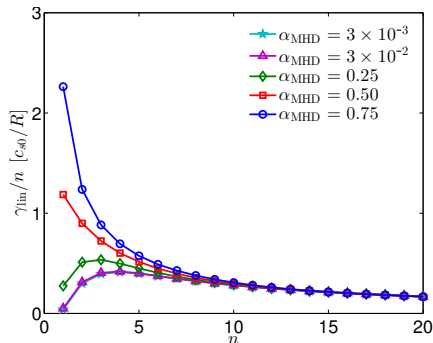
$$\partial p_{e1}/\partial r \sim \partial p_{e0}/\partial r \rightarrow p_{e1} \sim p_{e0}/(L_p k_r)$$

Estimating  $\phi_1 \sim \gamma_{\text{lin}}/(k_\theta k_r)$  and  $k_r \sim \sqrt{k_\theta/L_p}$  the radial flux is

$$\Gamma_r = \left\langle p_{e1} \frac{\partial \phi}{\partial \theta} \right\rangle \sim \frac{p_{e0}}{L_p} \frac{\gamma_{\text{lin}}}{k_r^2} \sim \frac{p_{e0}}{k_\theta} \gamma_{\text{lin}}$$

Global modes can drive large flux even if  $\gamma_{\text{lin}}$  is small

## Dominant mode number can be estimated with $\gamma_{\text{lin}}/n$

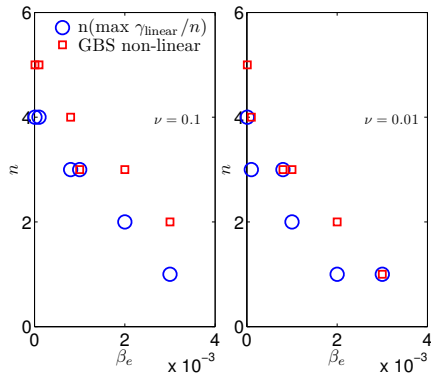


- Dominant  $n$  decreases as  $\beta_e$  increases

$$\Gamma \sim \gamma_{\text{lin}}/n \text{ dominated by } n \sim 1 \text{ for } \alpha_{\text{MHD}} \gtrsim 0.25$$

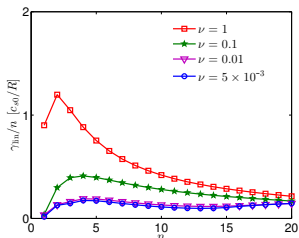
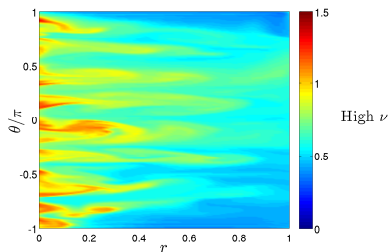
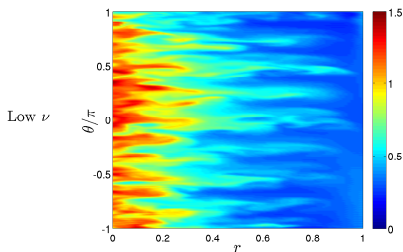


## $\Gamma \sim \gamma_{\text{lin}}/n$ matches dominant $n$ in GBS simulations



Downward trend can be explained by saturation mechanism

## Similar effect can be shown for $\nu$



▶ RBM unstable at high  $\nu$

▶  $\gamma_{lin}^2 \sim \frac{2R}{L_p} - \gamma_{lin} \frac{k_{\parallel}^2}{k_{\perp}^2 \nu} \rightarrow k_{\perp}^2 > \frac{k_{\parallel}^2}{\nu \sqrt{2R/L_p}}$

▶ Lower  $n \rightarrow$  global mode

## Conclusions

- ▶ Global 3-D, E+M simulations of SOL turbulence
  - ▶ Recovered  $R/L_p \sim 10-20$ , turbulent flux dominated by RBMs
  - ▶ Large fluctuation amplitude  $n_1/n_0 \sim O(1)$
  - ▶ Radially extended modes with  $k_r \sim \sqrt{k_\theta/L_p}$

3D non-linear global model required

- ▶ Dominant toroidal mode number vs.  $\beta_e$  or  $\nu$  consistent with flux estimate due to gradient removal mechanism  $\Gamma_r \sim \gamma/k_\theta$
- ▶ Shift toward global instability observed at high  $\beta_e$  and  $\nu$

Enhanced transport for high  $\nu$ ,  $\alpha_{\text{MHD}} \gtrsim 0.25$